Stable Equilibria of Satellites Containing a Momentum Wheel in a Controlled Gimbal

J. U. Beusch* and N. P. Smith†
Massachusetts Institute of Technology, Lexington, Mass.

In this paper are presented all stable equilibrium states of rotation of a rigid body satellite containing a single gimbaled momentum wheel in a zero gravity field. For an arbitrary but fixed speed of the wheel relative to the satellite body, it is shown that there may be one, two or three stable rotational equilibrium states of the satellite depending on the value of the total angular momentum. In each of these states the satellite body spins at a constant rate about an axis which is fixed in satellite coordinates. The relative orientation of this axis in both satellite and inertial coordinates can be determined from expressions in this paper. Expressions are also derived for the satellite angular velocities and angular position of the gimbal at each equilibrium state. The gimbal is actively controlled so that nutation damping occurs for all conditions of satellite unsteady rotation. In addition to extensive analog computer simulation studies, a prototype gimbal and momentum wheel system was designed and then tested on a spherical air bearing platform.

Nomenclature

B = gimbal viscous damping coefficient
C = center of mass of the entire vehicle-gimbal-wheel system
C_g = center of mass of wheel and gimbal assembly
$\bar{H}$ = angular momentum vector of satellite-wheel system with magnitude H
h = relative angular momentum of the wheel about its spin axis
I_1,I_2,I_3 = principal moments of inertia of wheel and gimbal assembly
$J_1,J_2,J_3,$ J_{12},J_{23},J_{31} = components of satellite vehicle inertia-tensor
K = gimbal torsional spring constant
K_1 = gimbal control system spring constant coefficient
K_2 = gimbal control system integral compensation coefficient
K_a = gimbal limit spring constant
S = LaPlace transform variable
T_c = nutation damping dominate time constant
y_1,y_2,y_3 = orthogonal wheel fixed reference frame
z_1,z_2,z_3 = orthogonal vehicle fixed reference frame
φ_n = magnitude of the nutation angle
θ = relative gimbal angle
θ_2,θ_3 = Euler angles defining the location of $\bar{H},\bar{\omega}$ in vehicle coordinates
$\bar{\omega}$ = angular velocity vector of satellite body, with magnitude $\omega = |\bar{\omega}|$
$\omega_1,\omega_2,\omega_3$ = vehicle angular rates about z_1,z_2,z_3, respectively

Introduction

SEVERAL papers have been written on various aspects of the analysis of single gimbal momentum wheel systems for the stabilization and orientation of a satellite vehicle. References 1–3 consider the stability about the zero gimbal angle state (nominal equilibrium state). In each of these papers the system is composed of a single momentum wheel mounted on a gimbal axis parallel to a principal axis and restrained by a linear spring and viscous damping torque proportional to gimbal angular rate. In Ref. 4 all the stable equilibria of a vehicle containing a single momentum wheel with spin axis fixed in body coordinates are determined. The spin axis is not necessarily parallel to a principal axis. In Ref. 5 the necessary conditions for the vehicle to convert to the zero gimbal angle state are derived. Conditions for other possible stable states were not considered as the system was to be designed such that the vehicle would most likely convert to the zero gimbal angle state. In this paper are presented all possible stable equilibria for a single gimbaled momentum wheel system where the gimbal is coupled to the vehicle with a linear torsional spring and viscous damping torque proportional to gimbal angular rate as shown in Fig. 1. The damping torque and part of the spring torque are provided by an active control system.

To the knowledge of the authors there has been no previous analysis published concerning all of the stable equilibria of a satellite containing a single gimbaled momentum wheel. Five cases of principal vehicle inertia configurations are

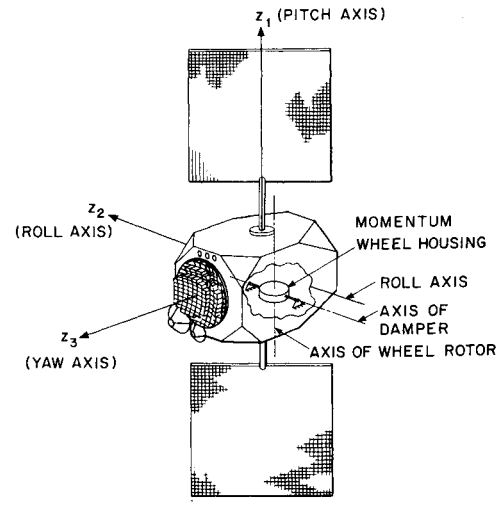

Fig. 1 Satellite vehicle and gimbaled momentum wheel.

Presented as Paper 70-1123 at the AIAA Guidance, Control and Flight Mechanics Conference, Santa Barbara, Calif., August 17–19, 1970; submitted August 19, 1970; revision received February 8, 1971. The authors are indebed to S. H. Wright, Leader, Control Systems Group, and C. Sullivan, Staff Member, Mechanical Engineering Group, M.I.T., Lincoln Laboratory, for several valuable suggestions and ideas concerning the work in this paper. This work was sponsored by the Department of the Air Force.

* Staff Member, Air Traffic Control Group. Member AIAA.
† Staff Member, Control Systems Group.

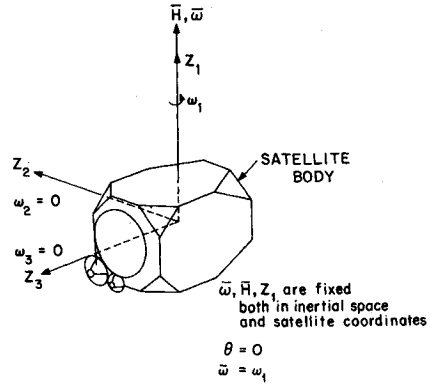

Fig. 2 State 1 equilibrium direction of H and ω in vehicle coordinates.

treated. In each case the momentum wheel spin axis is parallel to the axis of minimum, intermediate, or maximum principal inertia. The necessary conditions for stability of each equilibrium are given in terms of the parameters h, H, J_i, K, where the value of H is determined by the system initial conditions since momentum is conserved. The relative orientation of H in vehicle coordinates is defined by equations at each equilibrium state and is illustrated in Figs. 2–5. A method of achieving good nutation damping performance for this system is to minimize the expression for the damping dominant time constant T_c derived here. An actual prototype gimbal design and its control system is described. Analog simulation data and air bearing tests were used to verify the existance of predicted stable equilibria and validate the predicted nutation decay time performance.

System Description

The gimbaled momentum-wheel orientation and stabilization system, as originally conceived as a means of stabilizing a vehicle in space,[1] is based upon the principle of conservation of angular momentum in the absence of external torques. In the system considered here, the gimbal axis is coupled to the vehicle through two linear torsion springs located so one is at each end of the gimbal axis. These springs allow the gimbal to rotate relative to the vehicle about the gimbal axis only. Nutation damping is obtained by applying a viscous damping torque proportional to the relative gimbal rate.

Prior to ejection of the vehicle from the booster transtage, the momentum wheel is spun up to a fixed speed. After separation, the total system angular momentum vector $\bar{H}$ is fixed

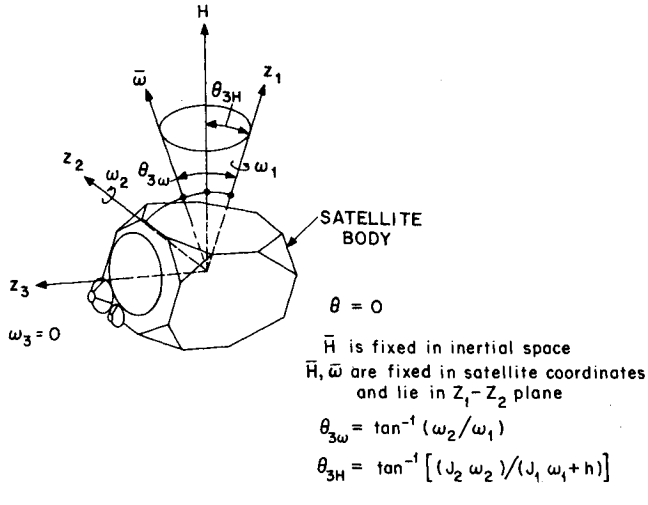

Fig. 3 State 2 equilibrium direction of H and ω in vehicle coordinates.

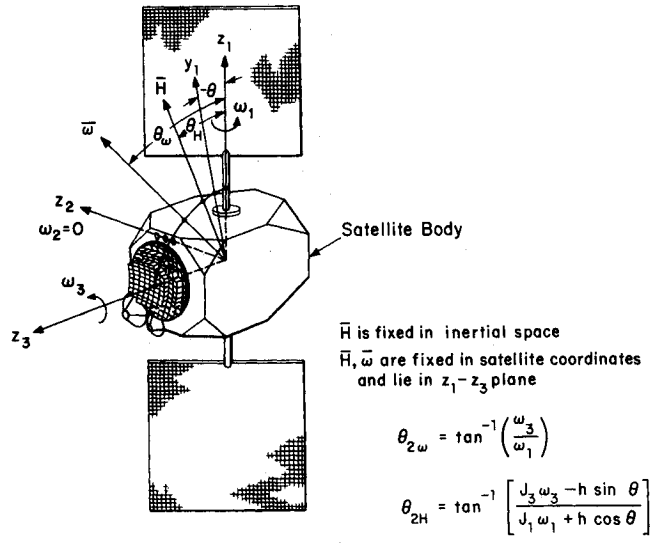

Fig. 4 State 3 equilibrium direction of H and ω in vehicle coordinates.

in inertial coordinates. Its magnitude and orientation are determined by the wheel speed and angular momentum due to angular "tip off" rates imparted at ejection. Immediately following separation, $\bar{H}$ is not fixed in vehicle coordinates due to the angular "tip off" rates. However, after the gimbal is uncaged, relative gimbal motion occurs and the gimbal control system provides viscous nutation damping proportional to relative gimbal motion so that the vehicle is driven to its stable equilibrium state, with $\bar{H}$ fixed in both vehicle and inertial coordinates.

The precise evaluation of the equilibrium conditions of this paper requires a knowledge of H, the magnitude of the angular momentum vector. Approximate bounds on the value of H can be determined from knowledge of the transtage and separation systems at vehicle ejection into orbit. In many cases, the equilibrium conditions are insensitive to fairly large variations in H. Therefore the results of this paper are useful when H is known only approximately.

Rotational Equations of Motion

In this section the satellite rotational equations of motion and equilibrium conditions are presented. The derivation parallels that of Ref. 5 and only the results are stated for the

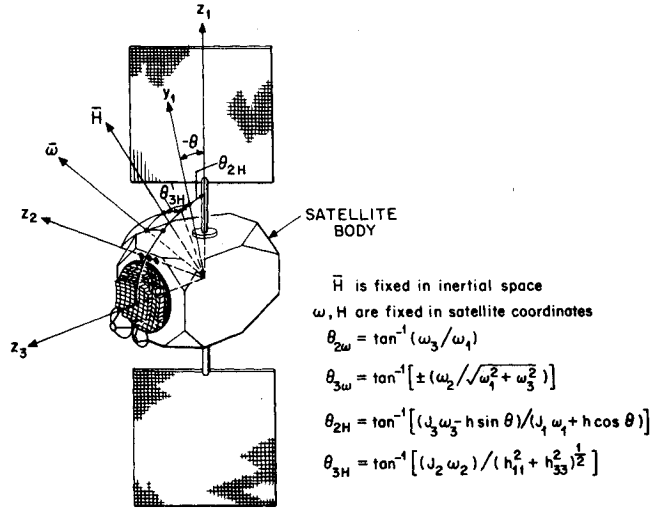

Fig. 5 State 4 equilibrium direction of H and ω in vehicle coordinates.

convenience of the reader. The "vehicle" subsystem excludes the gimbal and momentum wheel. Figure 6 shows the vehicle, gimbal, and wheel configuration. The general rotational equations of motion are derived, with the following assumptions.

1) An orthogonal vehicle-fixed reference frame (z_1,z_2,z_3) is chosen. An orthogonal, gimbal-fixed frame (y_1,y_2,y_3) is chosen such that the gimbal can rotate with respect to the vehicle about y_2, which is parallel with z_2. For $\theta = 0$, y_1 and y_3 are parallel to z_1 and z_3, respectively. The momentum wheel spin axis is parallel to y_1.

2) The center of mass of the momentum wheel lies on the wheel spin axis (i.e., the wheel rotor is balanced). The combined center of mass of the wheel and gimbal assembly C_g lies on y_2 so that the center of mass of the entire vehicle-gimbal-wheel system C is stationary within the vehicle frame. All components are assumed rigid elements. The physical location of y_2 is arbitrary within the vehicle.

3) The gimbal reference frame coordinates (y_1,y_2,y_3) are parallel to the principal axes of inertia of the gimbal-and-wheel subsystem, which has principal moments of inertia (I_1,I_2,I_3) about C_g.

4) The main vehicle inertias (J_1,J_2,J_3) are taken about C, the composite center of mass of the vehicle, gimbal and wheel system, and include the inertia of the gimbal and wheel, which are represented by a mass concentrated at C_g. These inertias are calculated about axes parallel to z_1,z_2,z_3 and centered on C. The changes of inertias due to deformation of the gimbal pivot spring and gimbal are neglected.

5) The magnitude of the relative angular momentum of the wheel about the wheel spin axis, as seen by an observer attached to (y_1,y_2,y_3), is h, which is held constant by a motor driven in a control loop by a tachometer.

6) There are no external torques. Thus momentum is conserved during the period of time for which the analysis holds.

With these six assumptions, Euler's moment equations for this system are

$$J_1\dot{\omega}_1 + J_{12}(\dot{\omega}_2 - \omega_1\omega_3) + J_{13}(\dot{\omega}_3 + \omega_1\omega_2) + J_{23}(\omega_2^2 - \omega_3^2) - (\dot{\theta} + \omega_2)(h\sin\theta + I_2\omega_2) + (J_3 - J_2)\omega_2\omega_3 + \dot{\omega}_1(I_1\cos^2\theta + I_3\sin^2\theta) + 0.5(\dot{\omega}_3 + \omega_1\omega_2)(I_3 - I_1)\sin 2\theta + \omega_2\omega_3(I_1\sin^2\theta + I_3\cos^2\theta) + (I_3 - I_1)\dot{\theta}(\omega_1\sin 2\theta + \omega_3\cos 2\theta) = 0 \quad (1)$$

$$J_2\dot{\omega}_2 + J_{12}(\dot{\omega}_1 + \omega_2\omega_3) + J_{23}(\dot{\omega}_3 - \omega_1\omega_2) + J_{13}(\omega_3^2 - \omega_1^2) + h(\omega_3\cos\theta + \omega_1\sin\theta) + (J_1 - J_3)\omega_1\omega_3 + I_2(\dot{\omega}_2 + \ddot{\theta}) + (I_1 - I_3)\times[\omega_1\omega_3\cos 2\theta + 0.5(\omega_1^2 - \omega_3^2)\sin\theta] = 0 \quad (2)$$

$$J_3\dot{\omega}_3 + J_{13}(\dot{\omega}_1 - \omega_2\omega_3) + J_{23}(\dot{\omega}_2 + \omega_1\omega_3) + J_{12}(\omega_1^2 - \omega_2^2) - (\dot{\theta} + \omega_2)(h\cos\theta - I_2\omega_1) + (J_2 - J_1)\omega_1\omega_2 + \dot{\omega}_3(I_3\cos^2\theta + I_1\sin^2\theta) + 0.5(\dot{\omega}_1 - \omega_2\omega_3)(I_3 - I_1)\sin 2\theta - \omega_1\omega_2(I_1\cos^2\theta + I_3\sin^2\theta) + (I_3 - I_1)\dot{\theta}(\omega_1\cos 2\theta - \omega_3\sin 2\theta) = 0 \quad (3)$$

$$I_2(\dot{\omega}_2 + \ddot{\theta}) + B\dot{\theta} + K(\theta) + G(\theta) + h(\omega_3\cos\theta + \omega_1\sin\theta) + (I_1 - I_3)[\omega_1\omega_3\cos 2\theta + 0.5(\omega_1^2 - \omega_3^2)\sin 2\theta] = 0 \quad (4)$$

Equations (1–3) express conservation of total angular momentum and Eq. (4) is the momentum equation of the gimbal and wheel about the roll axis.

For the purpose of the analysis presented here, a simplified version of Eqs. (1–4) can be used. This version is obtained with these additional assumptions. 1) Gimbal and wheel inertias are neglected ($I_1 = I_2 = I_3 = 0$) and h is retained as the only momentum contribution of these components. It can be shown that if $I_i \ll J_i$, $i = 1,2,3$ then this assumption results in negligible change in the stable equilibria and very little in nutation damping performance. 2) z_1,z_2,z_3 are principal axes for the total system as defined previously in assumption 4. Thus the product of inertia terms vanish, i.e., $J_{12} = J_{23} = J_{13} = 0$. The effect of removing this assumption is examined below. With these assumptions, the following simplified equations of motion are obtained:

$$J_1\dot{\omega}_1 + (J_3 - J_2)\omega_2\omega_3 - (\dot{\theta} + \omega_2)h\sin\theta = 0 \quad (5)$$

$$J_2\dot{\omega}_2 + (J_1 - J_3)\omega_1\omega_3 + h(\omega_3\cos\theta + \omega_1\sin\theta) = 0 \quad (6)$$

$$J_3\dot{\omega}_3 + (J_2 - J_1)\omega_1\omega_2 - (\dot{\theta} + \omega_2)h\cos\theta = 0 \quad (7)$$

$$B\dot{\theta} + K(\theta) + G(\theta) + h(\omega_3\cos\theta + \omega_1\sin\theta) = 0 \quad (8)$$

The function $K(\theta)$ designates the total gimbal torsional spring torque. One torsional spring supports the gimbal and provides a linear torque for small angles $|\theta| < \theta_{\max}$. The second spring is very stiff and acts as an elastic limit stop to maintain gimbal angles below a practical maximum value while still allowing relative angular motion. Thus $K(\theta)$ is represented mathematically by

$$K(\theta) = \begin{cases} K\theta \text{ for } |\theta| \leq \theta_{\max} \\ K\theta + K_a(\theta - \theta_{\max}) \text{ for } |\theta| > \theta_{\max} \end{cases} \quad (9)$$

The function $G(\theta)$ designates the torque generated by the gimbal torque motor in response to gimbal angular position feedback. The purpose of this torque is to provide nutation damping and accurate gimbal alignment by a feedback control system. A standard form of $G(\theta)$ is proportional plus integral feedback, i.e.,

$$G(\theta) = K_1\theta + K_2\int\theta dt \quad (10)$$

The parameters K_1, K_2 are easily adjusted to provide accurate gimbal nulling and to maintain a given gimbal spring constant. Unless otherwise noted, we shall assume K_1 is already included in K and that $K_2 = 0$. The effect of $K_2 \neq 0$ will be examined below.

In the steady state, $\dot{\omega}_1 = \dot{\omega}_2 = \dot{\omega}_3 = \dot{\theta} = 0$, so no energy is dissipated. Thus each of the possible steady state solutions of Eqs. (5–8) must satisfy

$$(J_3 - J_2)\omega_2\omega_3 - \omega_2 h\sin\theta = 0 \quad (11)$$

$$(J_1 - J_3)\omega_1\omega_3 + h(\omega_3\cos\theta + \omega_1\sin\theta) = 0 \quad (12)$$

$$(J_2 - J_1)\omega_1\omega_2 - \omega_2 h\cos\theta = 0 \quad (13)$$

$$K(\theta) + G(\theta) + h(\omega_3\cos\theta + \omega_1\sin\theta) = 0 \quad (14)$$

Stable equilibrium conditions are determined by applying the Routh-Hurwitz stability test to Eqs. (5–8) linearized about each steady-state solution satisfying Eqs. (11–14). These steady-state solutions are stable provided the total system energy E reaches a local minimum for all variations of $\omega_1,\omega_2,\omega_3,\theta$ which obey the angular momentum constraint $H =$ const, where

$$H^2 = (J_1\omega_1 + h\cos\theta)^2 + (J_2\omega_2)^2 + (J_3\omega_3 - h\sin\theta)^2 \quad (15)$$

Each steady-state solution for which the energy is minimum is a stable equilibrium state because no transition, without the addition of energy, can change this state. Another method used in determining the stable equilibrium conditions is to derive the first and second partial derivatives of E and H^2 in order to obtain the constrained first and second variations of the energy. These conditions so obtained are identical to those obtained from the Routh-Hurwitz criteria.

Stable Rotational Equilibrium States

This section presents the stable equilibrium solutions of Eqs. (5–8) for all values of H. For a given fixed set of parameter values, the attainable equilibrium states depend upon the value of total angular momentum H contained in the system. The value of H is constant and is determined by the vehicle initial conditions since angular momentum is conserved. As H is varied by changing the vehicle initial conditions, the system equilibrium states will change. In the following, whenever there is more than one stable equilibrium point for a given value of H (due to symmetry), only the particular initial conditions determine which point is reached. Here we specify each stable equilibrium state by the final relative orientation of the vehicle spin vector $\bar{\omega}$ which is fixed in satellite coordinates. We consider five cases of satellite principal inertia configuration. In each of the five cases treated, the stable equilibrium states attainable for all values of H are shown. The following conditions are necessary and sufficient for the stable equilibrium conditions to exist. Note that $H \geq 0$ and $h \geq 0$ since they are magnitude of vectors.

Case I $J_2 > J_1 \geq J_3$

In this case there are two stable equilibria possible. These equilibria are defined as states 1 and 2. The conditions required for the satellite to be in one or the other of these states are given below. If H satisfies the condition

$$H \leq J_2 h/(J_2 - J_1) \tag{16}$$

the stable equilibrium solution of Eqs. (5–8) is given by state 1, which is defined by

$$\omega_1 = (H - h)/J_1, \quad \omega_2 = \omega_3 = \theta = 0 \tag{17}$$

In this stable equilibrium state, the vehicle either does not spin or spins only about z_1, and the gimbal is centered ($\theta = 0$) as shown in Fig. 2. If H satisfies the condition

$$H > J_2 h_1/(J_2 - J_1) \tag{18}$$

the stable equilibrium solution of Eqs. (5–8) is given by state 2, which is defined by

$$\begin{aligned} &\omega_1 = h_1/(J_2 - J_1), \quad \omega_3 = \theta = 0, \\ &\omega_2 = \pm\{H^2 - [J_2 h_1/(J_2 - J_1)]^2\}^{1/2}/J_2 \end{aligned} \tag{19}$$

The vehicle spins about an axis in the z_1,z_2 plane and the gimbal is centered ($\theta = 0$) at equilibrium, as shown in Fig. 3. By symmetry there are two stable equilibria corresponding to positive and negative ω_2.

Case II $J_3 > J_1 \geq J_2$ **and Case III** $J_3 > J_2 > J_1$

In each of these cases there are two stable equilibria possible. These equilibria are state 1, defined by Eqs. (17) and state 3, defined here. The conditions on H for the system to be in either state 1 or 3 are given below. If H satisfies the condition

$$\begin{aligned} h - [J_1 K/(2h)]\{1 + &\{1 + (2h)^2/[K(J_3 - J_1)]\}^{1/2}\} < H < h - \\ &[J_1 K/(2h)]\{1 - \{1 + (2h)^2/[K(J_3 - J_1)]\}^{1/2}\} \end{aligned} \tag{20}$$

the stable equilibrium solution is given by state 1 as defined in Eqs. (17). If H satisfies either one of the following two conditions

$$0 < H \leq h - [J_1 K/(2h)]\{1 + \{1 + (2h)^2/[K(J_3 - J_1)]\}^{1/2}\} \tag{21}$$

$$H \geq h - [J_1 K/(2h)]\{1 - \{1 + (2h)^2/[K(J_3 - J_1)]\}^{1/2}\} \tag{22}$$

the stable equilibrium solution of Eqs. (5–8) is given by state 3, which is defined by

$$\omega_1 = -[K\theta/(2h \sin\theta)]\{1 \mp \{1 + (2h)^2 \sin\theta \cos\theta/[K\theta(J_3 - J_1)]\}^{1/2}\} \tag{23a}$$

$$\omega_2 = 0 \tag{23b}$$

$$\omega_3 = -[K\theta/(2h \cos\theta)][1 \pm [1 + (2h)^2 \sin\theta \cos\theta/(K\theta\{J_3 - J_1\})]]^{1/2} \tag{23c}$$

$$H^2 = (J_1\omega_1 + h \cos\theta)^2 + (J_3\omega_3 - h \sin\theta)^2 \tag{23d}$$

An explicit analytical solution for θ cannot be obtained in general for this case. A numerical solution for θ can be obtained by solving the transcendental equation obtained after elimination of ω_1 and ω_3 from Eqs. (23). In state 3, the vehicle spins about an axis in the z_1z_3 plane and the gimbal is not centered at equilibrium, as shown in Fig. 4. By symmetry, there are two stable equilibria corresponding to positive and negative ω_3. Note that condition (21) is satisfied only when the value of K satisfies the relation

$$K < h^2(J_3 - J_1)/(J_1 J_3) \tag{24}$$

Case IV $J_2 > J_3 > J_1$

In this case there are either two or three stable equilibria possible. If the gimbal spring constant K is larger than a given threshold, there are two stable equilibria for all values of H, [states 1 and 2 as defined by Eqs. (17) and (19)]. This case is identical to Case I. If K is smaller than the threshold value, there are three possible stable equilibria for all H. These three equilibria are states 1 and 3, defined by relations (17) and (23), respectively, and state 4 defined here. If K satisfies the condition

$$K \geq (J_3 - J_1)h^2/(J_2 - J_1)(J_2 - J_3) \tag{25}$$

the results of Case I are valid for Case IV. This means that if H satisfies condition (16) then the stable equilibrium solution is given by state 1 defined by Eqs. (17). If conditions (25) and (18) are satisfied, then the stable equilibrium solution is given by state 2 defined by Eqs. (19). If K satisfies the condition

$$0 < K < (J_3 - J_1)h^2/(J_2 - J_1)(J_2 - J_3) \tag{26}$$

and H satisfies condition (20), the stable equilibrium solution is given by state 1 defined by Eqs. (17). If K satisfies relation (26) and H satisfies either condition (21) or (22) and the relation

$$H \leq hJ_2[\cos^2\theta/(J_2 - J_1)^2 + \sin^2\theta/(J_2 - J_3)^2]^{1/2} \tag{27}$$

the stable equilibrium solution of Eqs. (5–8) are given by state 3. The value of θ in the upper bound of relation (27) is determined from the expression

$$K\theta - [h^2 \sin\theta \cos\theta(J_3 - J_1)/(J_2 - J_1)(J_2 - J_3)] = 0 \tag{28}$$

If K satisfies condition (26) and H satisfies

$$H > hJ_2[\cos^2\theta/(J_2 - J_1)^2 + \sin^2\theta/(J_2 - J_3)^2]^{1/2} \tag{29}$$

the stable equilibrium solution of Eqs. (5–8) is given by state 4, which is defined by

$$\begin{aligned} &\omega_1 = h \cos\theta/(J_2 - J_1), \quad \omega_3 = -h \sin\theta/(J_2 - J_3) \\ &\omega_2 = \pm\{H^2/J_2 - [h \cos\theta/(J_2 - J_1)]^2 - [h \sin\theta/(J_2 - J_3)]^2\} \end{aligned} \tag{30}$$

The value of θ in Eqs. (29) and (30) is determined from Eq. (28). In state 4 the vehicle spins about an axis which is in neither the z_1z_2 nor z_1z_3 planes, and the gimbal is not centered ($\theta \neq 0$) as shown in Fig. 6. By symmetry there are four stable

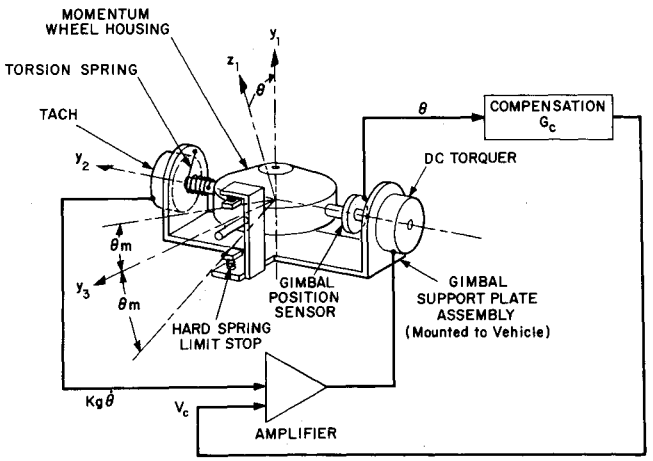

Fig. 6 Momentum wheel and gimbal control system schematic.

equilibria depending upon the signs of ω_3 and ω_2. A special case, which was not explicitly treated here, is that where $J_2 = J_3 > J_1$. This case is treated in Ref. 2.

Case V $J_1 \geq J_2 \geq J_3$

There is only one stable equilibrium state (state 1) and it is given by Eqs. (17) as shown in Fig. 2. Similar results are obtained if $J_1 \geq J_3 > J_2$. If $(J_1\omega_1 + h) < 0$, the z_1 component of H is initially negative. The vehicle z_1 axis will rotate 180° with respect to inertial coordinates so that the z_1 component of H is positive in its stable equilibrium state 1. If $H = 0$, the gimbal system provides little or no damping in the unsteady state. In practice, vehicle structural damping will dissipate energy so the vehicle will slowly convert to state 1.

Gimbal Control System

We have now determined all possible stable rotational states of the vehicle-gimbal-wheel system for a wide range of initial conditions and inertia configurations. The gimbal active control system, with relative gimbal rate and position feedback, provide the necessary damping and spring restraining torques to effectively damp out all unsteady motion (nutations) arising from initial conditions and drive the system to a stable equilibrium state. A method of parameter selection in the gimbal feedback control system to achieve acceptable nutation decay times for motion about each equilibrium state is given here. Other techniques are described in Refs. 1, 2 and 5.

We present an analytical expression for the vehicle nutation damping dominate time constant T_c (the time required for nutations to decay 63%) for the linearized case of motion near equilibrium state 1. Minimization of T_c was the method used in obtaining design parameter values for acceptable nutation damping performance. The damping performance predicted was then verified by analog simulation of the nonlinear equations of motion for a wide range of initial conditions. Coulomb friction in the gimbal has the effect of freezing the gimbal angle θ at a small value which allows a minimum nutation angle to exist. An expression for an upper bound on this angle is given. A brief description of a prototype gimbal design, which was developed and tested on a spherical air-bearing table, is included. Some of the mechanical and electrical problems encountered in this design are described. Also described is the effect of introducing a small amount of integral feedback into the gimbal control system to provide zero steady-state gimbal angle. This has the effect of reducing the number of stable equilibrium states possible for this system.

Nutation Damping Time Constant for State 1

The normal stable equilibrium state of the vehicle for most typical initial vehicle conditions is state 1 defined by Eqs. (17). This is a stable equilibrium state for all cases of inertia configuration and is expected to be the final state after a normal vehicle ejection in orbit. Linearizing Eqs. (5–8) about state 1 and taking LaPlace transforms, we obtain the characteristic equation

$$a_3S^3 + a_2S^2 + a_1S + a_0 = 0 \tag{31}$$

where

$$a_3 = BJ_2J_3, \quad a_2 = J_2[h^2 + J_3K + hJ_3(H - h)/J_1]$$

$$a_1 = B[J_2h - H(J_2 - J_1)][J_3h - H(J_3 - J_1)]/J_1^2$$

$$a_0 = [J_2h - H(J_2 - J_1)]\{K[J_3h - H(J_3 - J_1)] - h(J_3 - J_1)(H - h)^2/J_1^2\}/J_1$$

and H is determined by the initial conditions. Note that Eq. (31) is stable in each of the inertia configuration Cases I–V for values of H satisfying either condition (16) or (20). Approximate roots of Eq. (31) were derived. From the complex pair of roots which represent the oscillitory nutational motion, an approximate expression for the dominate time constant of Eq. (31) is

$$T_c = 2J_2[(J_1 - J_3)h^2 + J_1J_3K + J_3hH]^2/[(J_1Bh^2)\{J_2h + (J_1 - J_2)H\}]H \tag{32}$$

It has been verified that Eq. (32) is true when

$$\infty > T_c \gg [2BJ_1J_3]/[(J_1 - J_3)h^2 + J_1J_3K + J_3hH] \tag{33}$$

Equation (32) shows that the dominant nutation decay time constant near state 1 can be decreased by increasing the value of B or decreasing the value of K as long as Eq. (33) is not violated. A complete analysis of this type of damper using an integral squared error performance index is given in Ref. 5.

Coulomb Friction in Gimbal

When coulomb friction is present on the gimbal axis, it opposes gimbal relative motion $\dot{\theta}$ so that motion is prevented for small nutations and the gimbal does no damping. One of the major design goals in perfecting a prototype gimbal assembly capable of nearly perfect nutation damping was to reduce coulomb friction to a negligible value. This goal was accomplished in a prototype assembly as described later in this section.

The magnitude of the nutation angle φ_n, for which the gimbal does no damping due to the coulomb friction torque T_s, is bounded by the relation

$$|\varphi_n| < |T_s|(J_2J_3)^{1/2}/h^2 \tag{34}$$

Because of coulomb friction the equilibrium position of the gimbal in state 1 will not necessarily be $\theta = 0$. Increasing K and B reduces this problem at the expense of increasing T_c. Simultaneously increasing K and B reduces this effect with no decrease in T_c, but there is a practical limit due to amplifier gain limits and saturation effects as B becomes large, as well as the limit of Eq. (33). The approach taken was to use integral compensation in the gimbal position control system to maintain a steady-state gimbal null position.

Gimbal Integral Compensation

It was recognized early in the gimbal assembly design state that difficult practical problems were involved in obtaining a repeatable, accurate gimbal null position at steady state. Among these problems were coulomb friction effects, amplifier offset and drift with temperature and radiation, accurate null alignment and hysteresis of the gimbal torsional springs in a

zero gravity environment, and magnetic bias torques from the brushless dc torquer and tachometer. To minimize these problems, the integral compensation term defined by Eq. (10) was included in the gimbal control system. The effect of this compensation is to permit only those stable equilibrium solutions of Eqs. (5–8) with $\theta = 0$. This compensation reduces the number of stable equilibria from four possible states to three by eliminating states 3 and 4 and causing the addition of a new stable equilibrium state 5 defined by

$$\omega_1 = \frac{h}{J_3 - J_1} \tag{35}$$

$$\omega_3 = \pm \left[\left(\frac{H}{J_3}\right)^2 - \frac{h}{J_3 - J_1}^2\right]^{1/2} = -\left(\frac{K_2}{h}\right)\int_0^\infty \theta\, dt$$

This state is a stable equilibrium for inertia configuration Cases II and III where H satisfies the condition, $H > J_3 h/(J_3 - J_1)$. Adding integral compensation also increases the nutation decay time. To insure that the gimbal control system position bandwidth is less than the gimbal rate loop bandwidth, we require $K_2 < K^2/B$. Standard control system design techniques can be used to determine the best value of K_2. The addition of integral compensation allows accurate nulling of θ if a suitable angular position sensor is used. A rotary variable differential transformer was selected due to its resolution, accuracy, and small size and weight and because it requires no contact between rotor and stator.

Vehicle Product of Inertia Effects

Suppose assumption 2 is removed so that there are products of inertia terms present in the equations of motion. These equations are identical to those obtained by assuming the gimbal axes are misaligned with the vehicle principal axes. Equilibrium solutions can be obtained from Eqs. (1–4) with $I_1 = I_2 = I_3 = 0$. It can be shown that near the nominal equilibrium state 1, product of inertia terms cause the vehicle spin axis to be neither parallel with the z_1 axis nor the momentum wheel spin axis. Thus there will be a fixed gimbal offset which depends upon the relative magnitude of the product of inertia terms present. Elimination or reduction of this offset can be accomplished with integral feedback compensation.

Analog Computer Simulation

The complete simulation of Eqs. (5–10) on an analog computer was performed to verify the predicted damping performance of Eq. (32). The stable equilibria predicted here were also verified by the simulation for all five cases of inertia configuration. The parameter values used in the simulation were selected on the basis of a communications satellite designed by M.I.T. Lincoln Laboratory, Ref. 6. These parameter values are approximately $J_1,J_2,J_3 = 50, 75, 57$ slug-ft^2; $h = 7.5$ ft-lb-sec; $B = 6.0$ ft-lb/rad/sec; $K = 0.28$ ft-lb/rad; $K_a = 10$ ft-lb/rad; $\theta_{max} = 13°$; $K_1 = 0.12$ ft-lb/rad; $K_2 = 0.003$ ft-lb/rad-sec; and $I_1 = I_2 = I_3 = 0.06$ slug-ft^2.

In this case J_1 is the minimum inertia and there are three possible stable equilibria, any one of which the satellite can converge to, depending upon the satellite ejection initial conditions. A typical solution of $\omega_1,\omega_2,\omega_3,\theta$ vs time for a nominal satellite ejection of $H = 8.2$ ft-lb-sec is shown in Fig. 7. For this value of H stable equilibrium state 1 is reached in approximately 200 sec. Notice the effect of hard spring limiting on large values of θ in the gimbal response for $t < 30$ sec. Several hundred computer runs were made with various values of H to verify the expressions for the three

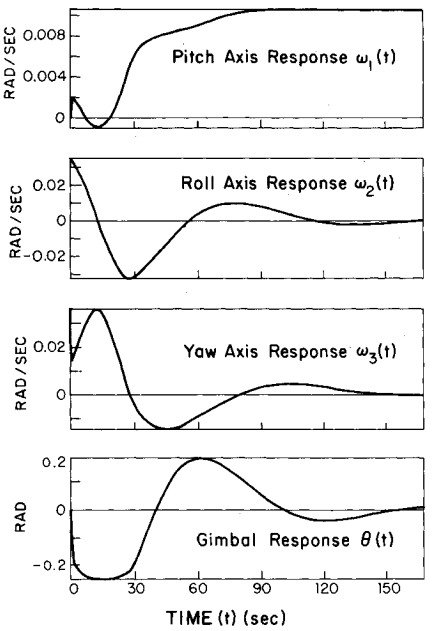

Fig. 7 Typical state 1 transient response for $H = 8.2$ ft-lb-sec.

stable equilibria predicted here and to obtain estimates of time required to reach these states. Substitution of the parameter values with $H = 8.2$ ft-lb-sec into relation (32) yields a damping time constant value of $T_c = 46$ sec, which agrees closely with the transient response of Fig. 7 as predicted.

It was also determined from the simulation data that the effect of the hard gimbal spring of Eq. (10) was to lengthen the damping time for large values of H by limiting the maximum excursion value of θ. If the steady-state value of θ approaches θ_{max} near state 3, there may be some ambiguity as to whether K satisfies condition Eq. (25) or (26) at the discontinuity point. For certain values of K, K_a, and H, this may result in an oscillatory settling condition as the vehicle approaches either state 3 or state 2. To eliminate this problem, the value of θ_{max} and K_a are selected so that for all practical values of H encountered, this situation will not occur.

Gimbal Design and Air Bearing Tests

A design utilizing passive gimbal control is shown in Ref. 7. However, this system was found to be too large and heavy for the LES-7 satellite. A prototype gimbal assembly was designed and fabricated by Lincoln Laboratory for evaluating the active gimbal control system concept as a vehicle nutation damper and attitude orientation device.[6] This design consists of a momentum wheel mounted in a support ring and suspended by two flex pivots. Total weight of the gimbal assembly without the wheel is 13.0 lb. This includes a caging device which can rigidly support the gimbal upon command from the ground. The prototype gimbal design used torsional pivot springs rather than bearings and was successful in eliminating, for practical purposes, coulomb friction torque.

There are several sources of bias torques in the gimbal assembly, but these presented no problem since they do not limit damping performance and will not cause θ to be nonzero in the steady state due to the integral compensation. Sources and bounds on the values of gimbal torque are as follows. Tachometer and torque motor magnetic bias torque is less than 0.06 oz-in. each. The gimbal sensor bias torque is less than 0.005 oz-in. The hard wire crossing device has a total torque of less than 0.02 oz-in.

Because of the nature of the gimbal torsional pivot springs which support the gimbal and wheel, there is an appreciable shift in the gimbal axis of rotation as the gimbal angle in-

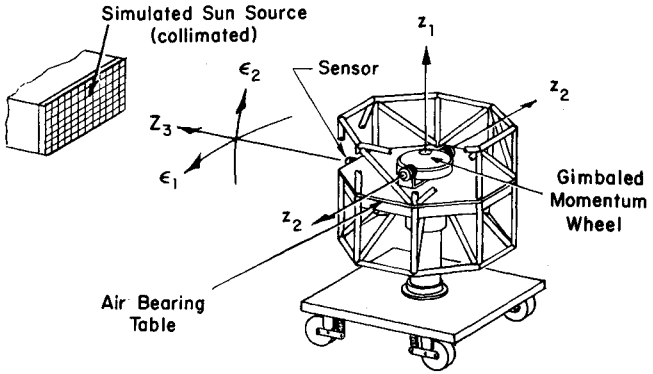

Fig. 8 Sketch of air bearing used for testing gimbal and vehicle dynamics.

creases. Allowances for this effect were made in the design and component selection to insure adequate linearity and null repeatability for controlling the gimbal angle to an accuracy of 0.1° under all expected operating conditions. Electrical power and tachometer signals for the wheel and motor are transmitted to the gimbal by a hard-wired device similar to that used in gyro designs.

The gimbal control system electronics consists of two feedback loops. The rate loop uses the gimbal tachometer output signal, which is highly amplified with a chopper stabilized preamplifier and fed to the power amplifier. The power amplifier provides a pulse width modulated output current whose average value is linear with the input voltage. The gimbal angle sensor output is linear with the input voltage. The gimbal angle sensor output is fed to digital compensation logic, which provides proportional plus integral compensation. This output is fed to a digital to analog converter and then is summed at the power amplifier input with the gimbal analog rate signal. Total power consumption for the system in the nominal state is less than 1 w. Peak power usage is limited to less than 12 w.

The prototype gimbal design has been functionally tested on a spherical air bearing platform as shown in Fig. 8. Platform inertias were built up to approximately 30 slug-ft^2 and the system was accurately balanced before testing. The gimbal was shown to quickly damp nutations of several degrees down to less than 0.1° in a few seconds. No major problems have been encountered and the design appears to be successful.

Conclusions

Inclusion of a gimbaled momentum wheel with active nutation damping in a satellite three-axis attitude control system greatly simplifies the design of the system. Because the damping rapidly drives the satellite to its stable equilibrium state, the dynamic behavior of the satellite that must be considered in control system design is greatly simplified. The results of this paper fall into two categories, design of the gimbal and damping control system and analysis of the dynamic behavior of the satellite in its stable equilibrium states. All possible states may be of interest because excessive disturbance torques due to tip off rates or unanticipated component failures, e.g., gas jets, could cause H to be larger than its nominal value. The first step in recovering from an excessive disturbance torque is understanding the important aspects of the dynamic behavior of the satellite under all conditions. The results of this paper provide this first step.

References

[1] Barker, A. C., "Momentum Bias Attitude Control for a Synchronous Communications Satellite," TOR-269(4540-70)-1, May 1964, Aerospace Corp., El Segundo, Calif.

[2] Karynov, A. A. and Kharitonova, T. V., "The Effects of External Perturbing Moments on the Dynamics of a Uniaxial Single-Flywheel Attitude Control System of a Spacecraft," *Prikladnaia Matematiki I Mekhanika*, Vol. 31, No. 6, May 22, 1967, pp. 1095–1103.

[3] Pringle, R., "On the Stability of a Body with Connected Moving Parts," *AIAA Journal*, Vol. 4, No. 8, Aug. 1966, pp. 1395–1403.

[4] Beusch, J. U., "Stable Equilibrium Orientation of a Spacecraft Which Contains a Momentum Wheel," TN-1967-16, Rev. 1, May 1968, M.I.T., Lincoln Lab., Lexington, Mass.

[5] Murray, F. T., Weinberger, M. R., and Graves, E. C., "Spring-Restrained, Momentum-Wheel Orientation and Stabilization System for Exoatmospheric Vehicles," *Journal of Spacecraft and Rockets*, Vol. 6, No. 4, April 1969, pp. 436–442.

[6] Beusch, J. U., Floyd, F. W., Much, C. H., Sferrino, V. J., and Smith, N. P., "Three-Axis Attitude Control of a Synchronous Communications Satellite," *AIAA Progress in Astronautics and Aeronautics: Communications Satellites for the 70's: Technology*, Vol. 25, 1971, p. 95, to be published.

[7] Hui, P. and Zaremba, J., "Implementation of a Semi-Active Gravity Gradient Controller," NASA Contractor report under Contracts NAS5-10253, NAS5-10453, 1968, TRW Systems, Redondo Beach, Calif.